DMD Fast Forward. Published on July 5, 2022 as DOI: 10.1124/dmd.122.000918
This article has not been copyedited and formatted. The final version may differ from this version.

THE COVID-19 ORAL DRUG MOLNUPIRAVIR IS A CES2 SUBSTRATE: POTENTIAL DRUG-DRUG INTERACTIONS AND IMPACT OF CES2 GENETIC POLYMORPHISM IN VITRO

Yue Shen[1], William Eades[1], William Liu[1], Bingfang Yan[1]*

[1]Division of Pharmaceutical Sciences, James L. Winkle College of Pharmacy, University of Cincinnati, Cincinnati, OH 45229, USA,

* To whom correspondence should be addressed.

Dr. Bingfang Yan
Division of Pharmaceutical Sciences
James L. Winkle College of Pharmacy
University of Cincinnati
Cincinnati, OH 45229

Running Title CES2-based hydrolysis of molnupiravir

* To whom correspondence should be addressed.

Dr. Bingfang Yan
Division of Pharmaceutical Sciences
James L. Winkle College of Pharmacy
University of Cincinnati
231 Albert Sabin Way
Cincinnati, OH 45229
Phone: (513) 558-6297, Fax: (513) 558-3233
E-mail: yanbg@uc.edu

Total number of manuscript pages	**48**
Number of figures	**7**
Number of tables	**3**
Word count of the Abstract	**243**
Word count of the Introduction	**744**
Word count of the Discussion	**1,500**

Abbreviation used: CES1, carboxylesterase-1; CES2, carboxylesterase-2; COVID-19, coronavirus disease of 2019; DMEM, Dulbecco's modified Eagle's medium; ENT1, equilibrative nucleoside transporter-1, ENT2, equilibrative nucleoside transporter-2, FBS, fetal bovine serum; ITS, insulin–transferrin–selenium; LC-MS/MS, liquid Chromatography with tandem mass spectrometry; RdRp, RNA-dependent RNA-polymerase, SARS-CoV-2 (severe acute respiratory syndrome coronavirus 2), and SDS-PAGE, sodium dodecyl sulfate-polyacrylamide gel electrophoresis.

DMD Fast Forward. Published on July 5, 2022 as DOI: 10.1124/dmd.122.000918
This article has not been copyedited and formatted. The final version may differ from this version.

Abstract. Molnupiravir is one of the two COVID-19 oral drugs that were recently granted the emergency use authorization by the Food and Drug Administration (FDA). Molnupiravir is an ester and requires hydrolysis to exert antiviral activity. Carboxylesterases constitute a class of hydrolases with high catalytic efficiency. Humans express two major carboxylesterases (CES1 and CES2) that differ in substrate specificity. Based on the structural characteristics of molnupiravir, this study was performed to test the hypothesis that molnupiravir is preferably hydrolyzed by CES2. Several complementary approaches were used to test this hypothesis. As many as 24 individual human liver samples were tested and the hydrolysis of molnupiravir was significantly correlated with the level of CES2 but not CES1. Microsomes from the intestine, kidney and liver but not lung all rapidly hydrolyzed molnupiravir and the magnitude of hydrolysis was related closely to the level of CES2 expression among these organs. Importantly, recombinant CES2 but not CES1 hydrolyzed molnupiravir, collectively establishing that molnupiravir is a CES2-selective substrate. In addition, several CES2 polymorphic variants (e.g., R180H) differed from the wild-type CES2 in the hydrolysis of molnupiravir. Molecular docking revealed that wild-type CES2 and its variant R180H used different sets of amino acids to interact with molnupiravir. Furthermore, molnupiravir hydrolysis was significantly inhibited by remdesivir, the first COVID-19 drug granted the full approval by the FDA. The results presented raise the possibility that CES2 expression and genetic variation may impact therapeutic efficacy in clinical situations and warrants further investigation.

DMD Fast Forward. Published on July 5, 2022 as DOI: 10.1124/dmd.122.000918
This article has not been copyedited and formatted. The final version may differ from this version.

Significance Statement. COVID-19 remains a global health crisis, and molnupiravir is one of the two recently approved oral COVID-19 therapeutics. In this study, we have shown that molnupiravir is hydrolytically activated by CES2, a major hydrolase whose activity is impacted by genetic polymorphic variants, disease mediators, and many potentially co-administered medicines. these results presented raise the possibility that CES2 expression and genetic variation may impact therapeutic efficacy in clinical situations and warrants further investigation.

Key words: COVID-19, molnupiravir, remdesivir, carboxylesterase-1 (CES1), caboxylesterase-2 (CES2), polymorphism.

DMD Fast Forward. Published on July 5, 2022 as DOI: 10.1124/dmd.122.000918
This article has not been copyedited and formatted. The final version may differ from this version.

1. INTRODUCTION

COVID-19 (coronavirus disease of 2019) continues to be a global health crisis [COVID-19 Dashboard, 2002; Asif et al., 2022]. Today, confirmed cases have surpassed 515 million with the death toll of over 6.3 million. SARS-CoV-2 (**s**evere **a**cute **r**espiratory **s**yndrome **co**rona**v**irus 2), the pathogen of COVID-19, belongs to the family of Coronaviridae [Asif et al., 2022]. COVID-19 vaccination has been shown to prevent infection and reduce severity, representing a significant stride in the scientific community and for the public health [Wagner et al., 2021]. So far, all approved vaccines target the Spike protein [COVID-19 Vaccines, 2022]. This protein is highly glycosylated, undergoes conformational changes and exhibit rapid mutations [Jia and Gong, 2021; Mansbach et al., 2021], contributing to waning immunity, breakthrough infection and multiple surges [Getz et al., 2021; Huang et al., 2021; Jia and Gong, 2021; Lipsitch et al., 2021; Mansbach et al., 2021].

The efforts of developing COVID-19 therapeutics, like those for vaccine development, are unprecedented [Ayele et al., 2021; Zhou et al., 2021]. In a short span of two years, more than dozens of therapeutic targets have been identified [Ayele et al., 2021; Zhou et al., 2021], and hundreds of clinical trials have been completed or under way [Coronavirus, 2022]. These targets represent a comprehensive list from directly inhibiting the replication of SARS-CoV-2, and to targeting the host protein TMPRSS2 (transmembrane protease, serine 2), a facilitator of SARS-CoV-2 infection [Ayele et al., 2021; Zhou et al., 2021]. The recent news from Merck and Pfizer is exciting. Both companies announce that they have developed oral pills (desirable formulation) with high efficacy [Coronavirus, 2022; New COVID, 2021]. The Merck pill molnupiravir reduces the risk of hospitalization and death from COVID-19 by 30%, whereas the Pfizer pill Paxlovid by 85% [Coronavirus, 2022; New COVID, 2021]. Paxlovid is a combination of the major ingredient nirmatrelvir and the boosting agent ritonavir [New COVID, 2021; Eng et al., 2022].

DMD Fast Forward. Published on July 5, 2022 as DOI: 10.1124/dmd.122.000918
This article has not been copyedited and formatted. The final version may differ from this version.

Mechanistically, nirmatrelvir inhibits SARS-CoV-2 replication by targeting the viral main protease (M^{pro}) [Zhao et al., 2021]. In contrast, molnupiravir, like the earlier approved COVID-19 drug remdesivir, inhibits viral replication by targeting RNA-dependent RNA-polymerase (RdRp) [Malone and Campbell, 2021; Zhang et al., 2021]. However, molnupiravir and remdesivir lead to different outcomes. Remdesivir causes RdRp to pause or induces chain termination, whereas molnupiravir causes RdRp to introduce widespread errors of the viral genome, leading to lethal mutagenesis. Importantly, $3CL^{pro}$ and RdRp, compared with the Spike protein, are more conserved [Bojkova et al., 2022; Muhammed et al., 2021; Showers et al., 2021; Waters et al., 2022]. For example, the Omicron isolates have only two missense mutations across the replicase-transcriptase complex [Bojkova et al., 2022]. RdRp, the core protein of the complex, has only a single mutation (i.e., P323L) [Bojkova et al., 2022]. This mutation is not in the RNA binding site and may not cause significant changes catalytically [Bojkova et al., 2022].

Both molnupiravir and remdesivir are ester prodrugs, initially hydrolyzed followed by phosphorylation to produce active metabolites (Fig. 1) [Imran et al., 2021; Yan et al., 2021]. Carboxylesterases constitute a class of hydrolases with high catalytic efficiency. In humans, CES1 and CES2 are two major **c**arboxyl**es**terases established to have profound pharmacological and toxicological significance [Holmes et al., 2010; Shen et al., 2019; Yan, 2012]. These two carboxylesterases, on the other hand, differ in their substrate specificity. CES1 preferably hydrolyzes esters with an acyl moiety relatively larger than its alkoxy moiety, whereas the opposite is true with CES2 [Shi et al., 2006, Tang et al., 2006; Wu et al., 2005]. Indeed, we have shown that remdesivir, with an acyl moiety relatively larger than its alkoxy moiety, is a robust CES1 substrate [Shen et al., 2021a]. Interestingly, we have also shown that remdesivir is a potent and irreversible CES2 inhibitor [Shen et al., 2021b].

DMD Fast Forward. Published on July 5, 2022 as DOI: 10.1124/dmd.122.000918
This article has not been copyedited and formatted. The final version may differ from this version.

In contrast to remdesivir, molnupiravir has an alkoxy moiety relatively larger than its acyl moiety (Fig. 1A). We therefore hypothesized that molnupiravir is preferably hydrolyzed by CES2. Several experiments were performed to test this hypothesis. Among individual human liver samples, the hydrolysis of molnupiravir was correlated significantly with the expression of CES2 but not CES1. Recombinant CES2 but not CES1 hydrolyzed molnupiravir. The hydrolysis of molnupiravir was inhibited by remdesivir, a potent and irreversible CES2 inhibitor [Shen et al., 2021b]. Furthermore, we have shown that some CES2 genetic polymorphic variants exhibited significantly altered activity toward molnupiravir. These results presented raise the possibility that CES2 expression and genetic variation may impact therapeutic efficacy in clinical situations and warrants further investigation.

DMD Fast Forward. Published on July 5, 2022 as DOI: 10.1124/dmd.122.000918
This article has not been copyedited and formatted. The final version may differ from this version.

2. MATERIALS AND METHODS

2.1. Chemicals and supplies

Molnupiravir and its hydrolytic metabolite N-hydroxycytidine were purchased from MedChem Express (Monmouth Junction, NJ). Remdesivir was from Synnovator Inc (Durham, NC). Raltegravir, structurally similar to molnupiravir, was from Astatech (Bristol, PA). 4-Methylumebelliferyl acetate was from Alfa Aesar (Tewksbury, MA). The goat anti-rabbit-IgG conjugated with horseradish peroxidase was from Sigma (Saint Louis, MO). Human liver, kidney, intestine and lung tissues or microsomes were from SEKISUI Xenotech (Kansas City, KS). DMEM (Dulbecco's modified Eagle's medium), ITS (insulin–transferrin–selenium), penicillin streptomycin solution (100x) were from Corning (Glendele, AZ). Collagen from rat tail were from Roche (Basel, Switzerland). Unless otherwise specified, all reagents were purchased from Thermo Fisher Scientific (Waltham, MA).

2.2. Hydrolysis of molnupiravir and LC-MS/MS analysis (liquid chromatography with tandem mass spectrometry)

Molnupiravir is an ester and hydrolysis is required to exert antiviral activity [Rosenke et al., 2021]. Carboxylesterases, a major class of hydrolases with high catalytic efficiency, are expressed in an organ-differential manner with the highest activity in the liver [Holmes et al., 2020; Xie et al., 2002]. The hydrolysis of molnupiravir was therefore performed by a large number of liver samples, microsomes from various organs and recombinant human carboxylesterases. The enzymatic assays were conducted as described elsewhere [Shi et al., 2006; Shen et al., 2021a]. All incubations were performed at 37°C in a total volume of 50 μL. Pilot studies were performed to determine conditions (e.g., protein concentrations) to maintain the metabolism in the linear range. Generally, S9 fractions (5 μg protein) were prepared in 25 μL of incubation buffer (Tris-HCl 50 mM, pH, 7.4) and then mixed with an equal volume of molnupiravir solution at a concentration of 2 μM (in the same buffer). To prepare S9 fractions,

DMD Fast Forward. Published on July 5, 2022 as DOI: 10.1124/dmd.122.000918
This article has not been copyedited and formatted. The final version may differ from this version.

liver tissue samples were homogenized in homogenization buffer (50 mM Tris-HCl, pH 7.4, 150 mM KCl, 2 mM EDTA) at a ratio of 1 g wet tissue per 4 mL and then centrifuged at 10, 000 *g* for 20 min. The supernatant was collected and determined for protein concentrations. The incubations lasted for 40 min, and the reactions were stopped with 100 μL termination buffer (acetonitrile : methanol = 3:1) containing the internal standard raltegravir (0.15 μM). The reaction mixtures were subjected to centrifugation at 12,000 *g* for 15 min at 4°C. As controls, the reactions were stopped at 0 min or carried out without protein.

Supernatants (8 μL) were analyzed for the hydrolysis by the LC-MS/MS system TSQ-FORTIS (Thermo Fisher Scientific, Waltham, MA). Analytes were separated by Chromolith SpeedROD RP-18 column at 40°C with a gradient mobile phase constituting (A) ammonium acetate (1 mM, pH 4,3) in water and (B) ammonium acetate (1 mM) in acetonitrile. The mobile phase gradient, at a flow rate of 1 mL/min, was generated as follows: 2% acetonitrile for the first 1.2 min, 2-90% for 1.3 min, 90-2% for 0.3 min and 2% for 2.2 min. The analytes were detected in negative ion mode using the following mass transitions: m/z 328.18 $\rightarrow$ 126.14 for molnupiravir, 258.1 $\rightarrow$ 126.04 for the hydrolytic metabolite N-hydroxycytidine and 443.2 $\rightarrow$ 316.18 for raltegravir. The assay was linear from 10 to 3000 ng/ml for molnupiravir and from 1 to 1000 ng/mL for N-hydroxycytidine. All quantifications were performed using peak area ratios, and the calibration curves consisted of molnupiravir or N-hydroxycytidine to raltegravir ratios plotted against the molnupiravir or N-hydroxycytidine to raltegravir peak area ratios.

2.3. Carboxylesterase activity by native gel-electrophoresis

We have shown that many carboxylesterases remain active in polyacrylamide gel [Shen et al., 2021b; Xiao et al., 2012]. Importantly, carboxylesterases, even hydrolyzing the same substrate, can be electrophoretically separated and individually determined for hydrolytic activity. As a

DMD Fast Forward. Published on July 5, 2022 as DOI: 10.1124/dmd.122.000918
This article has not been copyedited and formatted. The final version may differ from this version.

result, the relative inhibition between carboxylesterases (e.g., CES1 and CES2) can be specified on the same gel. In this study, two formats of inhibition were tested for the hydrolysis of molnupiravir including microsomes and primary hepatocytes. For the inhibition with subcellular fractions, human microsomes (2 μg) were incubated with remdesivir (0, 1, 10 μM) for 2 h in a total volume of 20 μL (50 mM Tris-HCl,150 mM KCl, 2mM EDTA, pH7.4). The incubations were then mixed with 5x sample buffer (1.25M Tris-HCl, 40% Glycerol, 0.04% Bromophenol Blue, pH 6.8), and then subjected to electrophoresis as described previously [Shen et al., 2021b; Xiao et al., 2012]. After electrophoresis, gels were washed in 100 mM potassium phosphate buffer (pH 6.5) for 3 times (10 min each), followed by incubating in the same buffer containing 4-methylumbelliferylacetate for 15 min. Images were captured by ChemiDoc Imaging system. To gain significance in intracellular setting, human primary hepatocytes were treated with remdesivir at various concentrations for 2 h. Cell lysates were prepared and analyzed for inhibition of carboxylesterase activity by native gel electrophoresis.

2-4. Inhibition of molnupiravir hydrolysis by remdesivir

We have reported that remdesivir, the first COVID-19 drug approved by the Food and Drug Administration, is a potent and irreversible CES2 inhibitor [Shen et al., 2021b]. Remdesivir was therefore tested for the inhibition of molnupiravir hydrolysis. Once again, two experimental formats were used: microsomes and primary hepatocytes. Microsomes (2 μg) were pretreated for 2 h with remdesivir at various concentrations (0, 1 and 10 μM) and then treated with molnupiravir (1 μM). The hydrolysis was monitored by LC-MS/MS as described above. For intracellular inhibition, cryopreserved hepatocytes from 3 individuals were pooled and cultured as suspensions in 80% William E medium supplement with 1x ITS, Glutenin, 0.1 μM dexamethasone and penicillin/streptomycin for 30 minutes. The hepatocytes were treated with remdesivir at various concentrations for 2 h, the mixtures were collected, centrifuged at 1000 *g* for 5 min, washed thoroughly, and then incubated with molnupiravir at 1 μM. The incubation

DMD Fast Forward. Published on July 5, 2022 as DOI: 10.1124/dmd.122.000918
This article has not been copyedited and formatted. The final version may differ from this version.

lasted for 40 min. The hepatocyte suspensions were centrifuged at 1000 *g* for 5 min. The supernatant was collected and mixed with termination buffer containing the internal standard raltegravir as described above. The cell pellets were mixed with 100 μL termination buffer and centrifuged at 12,000 *g*. The parent drug and its hydrolytic metabolite in the media and cells were determined by LC-MS/MS.

2-5. Transfection

Human embryonic kidney cells (293T) were plated at a density of 60% in DMEM supplemented with 10% fetal calf serum. After reaching 80% confluence, cells were transfected by Lipofectamine. A plasmid construct or the empty vector (2 μg/well in 6-well plate) was diluted in 150 μL of serum-free DMEM and then mixed with the same volume of diluted Lipofectamine reagent with the same medium. The mixture was incubated for 5 min and then applied to a monolayer of 293T cells. After a 24-h incubation, cells were rinsed and harvested in 1.5 mL of Tris-HCl buffer (50 mM, pH 7.4). The cell suspension was sonicated by a Branson Sonifier, and cell debris was removed by centrifugation at 12,000 *g* for 10 min at 4°C. The cloning of CES1 and CES2 as well as the site-directed mutagenesis variants were described in our previous publications [Zhu et al., 2000; Xiao et al., 2013].

2-6. Western blotting

Western blotting was performed essentially as described previously [Shen et al., 2020; Xie et al., 2002]. Tissue homogenates (microsomes or S9 fraction) and cell lysates were resolved by 7.5% SDS-PAGE in a mini-gel apparatus and transferred electrophoretically to nitrocellulose membranes. The membranes were then blocked in 5 % non-fat milk. The blots were incubated with an antibody against CES1, CES2, GAPDH or actin. The preparation of the antibodies against CES1 and CES2 was described elsewhere [Zhu et al., 2000]. In both cases, the antigens were synthetic peptides conjugated with keyhole limpet hemocyanin. The sequence of

DMD Fast Forward. Published on July 5, 2022 as DOI: 10.1124/dmd.122.000918
This article has not been copyedited and formatted. The final version may differ from this version.

CES2 peptide was H2NCEKPPQTEHIEL-COOH, and of CES2 was H_2N-CQELEEPEERHTEL-COOH. Their specificity was established by recombinant CES1 and CES2, respectively. The primary antibodies were subsequently localized with goat anti-rabbit IgG conjugated with horseradish peroxidase, and horseradish peroxidase activity was detected with a chemiluminescent kit. The chemiluminescent signals were captured by ChemiDoc Imaging system.

2-7. Molecular docking

The molecular docking of molnupiravir or remdesivir to CES2 and its variant R180H was performed by Autodock Vina [Trott et al., 2010]. The ligands were sourced from PubChem as 3-D spatial data files. The files were converted into PDB files (program database) using Open Babel [O'Boyle et al., 2011], and subsequently prepared with Autodock Tools for simulation as PDBQT files (Protein Data Bank, Partial Charge (Q), & Atom Type (T) [Morris et al., 2009]. A homology model of wild-type CES2 (ID: 000748) was downloaded from the PDB and Swiss Model websites (https://swissmodel.expasy.org/repository/uniprot/O00748) and cleaned to remove the ligand and any other unwanted molecules such as water using the Chimera [Bienert et al., 2017]. The CES2 mutant (i.e., R180H) was generated in the Chimera with the rotamer function [Shapovalov et al., 2011]. These files were then prepared for simulation by Autodock Tools. The center for the Autodock Vina simulation was the center of CES2 or its mutant. The search box was set to 126 x 126 x 126 with an exhaustiveness of 100.

2-7. Other assays

Protein concentration was determined with Micro BCA Reagent from Pierce as described by the manufacturer. Data are presented as mean ± S.D. of at least three separate experiments, except where results of blots are shown, in which case a representative experiment is depicted in the figures. Statistical analyses were performed with SPSS-PASW Statistics 18. Significant

DMD Fast Forward. Published on July 5, 2022 as DOI: 10.1124/dmd.122.000918
This article has not been copyedited and formatted. The final version may differ from this version.

differences were made for comparison of means according to One-way ANOVA followed by a DUNCAN's test or Student's t test wherever appropriate. Statistical significance was indicated by asterisk signs or in combination with a line when a *p* value was less than 0.05, 0.01 or 0.001.

DMD Fast Forward. Published on July 5, 2022 as DOI: 10.1124/dmd.122.000918
This article has not been copyedited and formatted. The final version may differ from this version.

3. RESULT

3.1. High correlation of molnupiravir hydrolysis with CES2 but not CES1 expression

Carboxylesterases are important hydrolases with high catalytic efficiency [Holmes et al., 2010; Shen et al., 2019; Yan, 2012]. Humans express two major carboxylesterases (i.e., CES1 and CES2) that have profound pharmacological and toxicological significance [Holmes et al., 2010; Shen et al., 2019; Yan, 2012]. CES1 preferably hydrolyzes esters with an acyl moiety relatively larger than its alkoxy moiety, whereas the opposite is true with CES2 [Shi et al., 2006, Tang et al., 2006; Wu et al., 2005]. As shown in Fig. 1A, molnupiravir has an acyl moiety (boxed) relatively smaller than its alkoxy moiety. The hydrolytic metabolite N-hydroxycytidine, on the other hand, differs from the parent drug molnupiravir in lipophilicity. Molnupiravir has an XLogP3 value of -0.8 whereas N-hydroxycytidine of -2.2 [https://pubchem.ncbi.nlm.nih.gov/compound/eidd-2801; https://pubchem.ncbi.nlm.nih.gov/compound/197020]. We therefore hypothesized that molnupiravir is a preferable CES2 substrate and differs from N-hydroxycytidine in the chromatographic elution profile. As shown in Figs. 1C and D, molnupiravir had a retention time of 2.74 min, whereas N-hydroxycytidine had a retention time of 0.81 min, confirming that molnupiravir is more lipophilic than N-hydroxycytidine.

To establish whether molnupiravir is preferably hydrolyzed by CES2, as many as 24 individual human liver S9 samples were tested for the hydrolysis and the magnitude of the hydrolysis was analyzed for the correlation with the expression of CES1 and CES2. Overall, all samples hydrolyzed molnupiravir and the hydrolysis showed approximately a 10-fold individual difference (Fig. 2A). Among these samples, CES1 showed an 8-fold individual variation and CES2 a 15-fold in terms of expression (Fig. 2B). Importantly, the level of CES2 was correlated well with the hydrolysis at a correlation coefficient of 0.693 (p = 0.0012). In contrast, the level of CES1 was correlated modestly with the hydrolysis at a much lower correlation coefficient: 0.216 (p = 0.0141). Nevertheless, there were outliers even for CES2 (arrowed). Interestingly, the level of

DMD Fast Forward. Published on July 5, 2022 as DOI: 10.1124/dmd.122.000918
This article has not been copyedited and formatted. The final version may differ from this version.

CES1 was correlated with the level of CES2 at a correlation coefficient of 0.506 (p = 0.0117), pointing to a potential co-regulation in their expression among these donors.

3.2. Molnupiravir hydrolysis by organ microsomes and recombinant CES1 and CES2

It has been reported that CES2 is abundantly expressed in the intestine, liver and kidney but not lung [Xie et al., 2002]. We next tested whether these organs differentially hydrolyze molnupiravir. Microsomes from these organs were pooled and analyzed for the hydrolysis of molnupiravir. As expected, microsomes from the intestine, liver and kidney but not lung robustly hydrolyzed molnupiravir (Fig. 3A). The relative activities toward molnupiravir were consistent with the relative expression of CES2 (Fig. 3A). The chromatogram showed robust presence of the hydrolytic metabolite N-hydroxycytidine upon incubation with intestinal microsomes (Fig. 3B). To further establish the dominant role of CES2 in molnupiravir hydrolysis, cells (293T) were transfected with CES1, CES2 or the corresponding vector and the cell lysates were tested for the hydrolysis of molnupiravir. As shown in Fig. 3C, lysates from CES2- but not CES1- or vector-transfected cells hydrolyzed molnupiravir. Western blotting confirmed the expression of CES1 and CES2 in their respectively transfected cells (Fig. 3C).

3.3. Inhibition of molnupiravir hydrolysis by remdesivir

We have reported that several drugs are potent and irreversible CES2 inhibitors including remdesivir, the first medicine approved for COVID-19 [Shen et al., 2021b; Shen and Yan, 2017; Xiao et al., 2013]. Next we tested whether remdesivir inhibits the hydrolysis of molnupiravir. Two experimental formats were used: microsomes and primary hepatocytes. Microsomes (2 μg) from various organs were pretreated for 2 h with remdesivir at 0, 1 or 10 μM and then incubated with molnupiravir (1 μM). The inhibition was monitored by native-gel electrophoresis-coupled activity-staining with 4-methylumbelliferylacetate as the substrate (in gel), and in parallel microsomal incubations, the hydrolysis of molnupiravir was monitored by LC-MS/MS. As

DMD Fast Forward. Published on July 5, 2022 as DOI: 10.1124/dmd.122.000918
This article has not been copyedited and formatted. The final version may differ from this version.

expected, liver microsomes produced three carboxylesterase bands (Fig. 4A). The top two were both CES1 (presumably different extent of glycosylation) and the band with the fastest migration was CES2. Importantly, CES2 but not CES1, as clearly shown by the liver microsomes, was catalytically inhibited by remdesivir and the inhibition occurred in a concentration-dependent manner (Fig. 4A). Consistent with the observed inhibition of CES2 by remdesivir, the hydrolysis of molnupiravir was significantly reduced (Fig. 4B). The hydrolysis by the intestinal microsomes was decreased by as much as 90% even at 1 μM remdesivir (Left of Fig. 4B). In contrast, the decrease of molnupiravir hydrolysis by liver microsomes was less profound. Remdesivir at 10 μM decreased the hydrolysis by 40% (Middle of Fig. 4B). As seen with intestinal microsomes, 1 and 10 μM remdesivir caused comparable inhibition of molnupiravir hydrolysis by kidney microsomes (~60%, Right of Fig. 4B).

To complement the microsomes-based approach, the intracellular inhibition was determined in cryopreserved hepatocytes. Donors-pooled hepatocytes were used. Hepatocytes were pretreated with remdesivir at various concentrations for 2 h, thoroughly washed, resuspended and then incubated with molnupiravir. Medium and hepatocytes were collected for the qualification of the hydrolytic metabolite. Cell lysates were also analyzed by native gel electrophoresis-coupled staining for confirming the inhibition of CES2 by remdesivir. The results are summarized in Fig. 5. As expected, remdesivir profoundly inhibited CES2 but not CES1 and the inhibition occurred in a concentration-dependent manner (Fig. 5A). On the other hand, the overall staining for CES2 and the sensitivity toward remdesivir inhibition varied depending on a donor. Sample from donor #7 showed the lowest staining (0 μM remdesivir) and the most resistant to remdesivir inhibition. In contrast, samples from donors 25 and 33 showed comparable staining (0 μM remdesivir) and the similar sensitivity to remdesivir (Fig. 5A). As for the hydrolysis of molnupiravir, hepatocytes from donor #7 (0 μM remdesivir), based on the total number of cells (10^6), produced the highest amount of N-hydroxycytidine, the hydrolytic

DMD Fast Forward. Published on July 5, 2022 as DOI: 10.1124/dmd.122.000918
This article has not been copyedited and formatted. The final version may differ from this version.

metabolite. This was true for all quantitative analyses for N-hydroxycytidine with an exception of its intracellular concentration when molnupiravir was incubated at 0 μM (Top of Fig. 5B). Consistent with the native-gel electrophoresis, sample from donor #7 was more resistant to remdesivir inhibition in terms of molnupiravir than those from donors #25 or #33 (Figs. 5B and C). Overall, incubation with a lower concentration of molnupiravir, namely at a concentration of 1 verse 5 μM, produced a less amount of N-hydroxycytidine (Top versus Bottom of Figs. 5B and C). Also, the extracellular concentration was 100- to 200-fold as much as the intracellular concentration depending on the incubation concentration of molnupiravir (Figs. 5B and C). Interestingly, the inhibition of molnupiravir hydrolysis was more robust in hepatocytes than that in liver microsomes, there were two major possibilities: (1) the liver microsomes have high levels of CES1, which robustly hydrolyzed remdesivir, leading to decreased inhibitory potency; and (2) hepatocytes had higher levels of CES2 (microsomal and cytosolic as shown in Fig. 5A), leading to a relatively greater inhibition (the more the sensitive target exists, the more inhibition). Indeed, Fig. 4A (liver microsomes) showed a greater activity staining of CES1 than CES2, whereas Fig. 5A (hepatocytes) showed a greater staining of CES2 than CES1.

3.4. Hydrolytic activation of molnupiravir by CES2 polymorphic variants

We have reported CES2 polymorphic variants that show altered catalytic activity and/or sensitivity to inhibitors [Xiao et al., 2013]. We next tested whether some of the variants differ from the wild-type CES2 in the hydrolysis of molnupiravir and/or the resistance to remdesivir-inhibition. Cells (293T) were transfected with a CES2 plasmid construct or the empty vector, and the cell lysates were tested for the hydrolysis of molnupiravir. As shown in Fig. 5A, Western blotting detected robust expression of wild-type CES2 and its variants with an ~20% difference. Based on the normalization with Western blotting, the variants A139T and L45I hydrolyzed molnupiravir comparably as the wild-type CES2. On the other hand, the variants A178V and F485V showed decreased hydrolysis compared with the wild-type CES2 by 74 and

DMD Fast Forward. Published on July 5, 2022 as DOI: 10.1124/dmd.122.000918
This article has not been copyedited and formatted. The final version may differ from this version.

61%, respectively. In contrast, the variant R180H, compared with the wild-type, showed much higher hydrolytic activity toward molnupiravir. In fact, this variant was 77% more active than the wild-type CES2 (Fig. 5A).

Next we tested whether these variants differ from the wild-type CES2 in remdesivir-mediated inhibition of molnupiravir hydrolysis. As described with microsomes and hepatocytes, lysates from transfected cells were treated with remdesivir at various concentrations (0, 0.1, 1 and 10 μM), and the remaining activity toward molnupiravir was determined. As shown in Fig. 5B, remdesivir at 0.1 μM inhibited the wild-type CES2 for hydrolysis of molnupiravir by as much as 87%, representing the highest inhibition among all recombinant CES2 (Fig. 5B). Increased remdesivir concentration such as 1 μM caused additional inhibition from 87 to 92%. Interestingly, some variants were as sensitive as the wild-type CES2 to the inhibition of remdesivir at 1 μM. However, they were more resistant to 0.1 μM remdesivir. For example, remdesivir at 0.1 μM inhibited the variant R180H by 65% but as much as 97% at 1 μM. This variant was the most active variant in terms of molnupiravir hydrolysis.

3.5. Molecular docking

We have shown that molnupiravir was a CES2 substrate, whereas remdesivir was a CES2 irreversible inhibitor (Figs. 2, 3, 4 and 5). We have also shown that the CES2 variant R180H, compared with the wild-type CES2, was more active to molnupiravir but more resistant to remdesivir (i.e., 0.1 μM) (Fig. 6A). To gain structural insight, we performed docking study. As shown in Fig. 7 and Table 1, both molnupiravir and remdesivir made contacts with CES2 and its variant R180H through Van der Waals force, hydrogen bond, pi-sigma, pi-alkyl and pi-cation interactions. Overall, molnupiravir used relatively more Van der Waals force and hydrogen bond in its interactions, whereas remdesivir used relatively more pi-sigma, pi-alkyl and pi-cation in its interactions (Fig. 7). Such differences were probably due to the difference in their

DMD Fast Forward. Published on July 5, 2022 as DOI: 10.1124/dmd.122.000918
This article has not been copyedited and formatted. The final version may differ from this version.

chemical structure. Remdesivir but not molnupiravir has multiple ring systems (Fig. 1A) [Shen et al., 2021b].

As shown in Fig. 7 and Table 1, molnupiravir made contacts with CES2 through 17 amino acids, whereas remdesivir through 19 amino acids. Importantly, as many as 13 amino acids were shared by molnupiravir and remdesivir for the interaction including: L258, G261, H322, Q324, L379, M380, S414, I418, P419, Q422, W538, K539 and L542. With exceptions of 5 amino acids, all shared residues used the same types of interaction. For example, Q422 interacted with molnupiravir and remdesivir via hydrogen bond. Conversely, H322 interacted with molnupiravir via Van der Waals force but pi-cation with remdesivir. Likewise, molnupiravir and remdesivir shared a large number of amino acids (14 in total) for the interaction with the variant R180H (Fig. 7, Table 1). Among them, with exceptions of L257 and I263, were those shared by molnupiravir and remdesivir for the interaction with the wild-type CES2. As for the interaction with molnupiravir between the wild-type CES2 and the variant R180H, there were as many as 9 different amino acids including: A257, P260, L262, I263, L378, P323, M415, L381 and K539. In contrast, only 3 amino acids (A257, S266 and L381) were different between the wild-type and the variant in interacting with remdesivir.

DMD Fast Forward. Published on July 5, 2022 as DOI: 10.1124/dmd.122.000918
This article has not been copyedited and formatted. The final version may differ from this version.

4. DISCUSSION

The efforts of developing COVID-19 therapeutics are massive and unprecedented [COVID-19 Vaccines 2022; Ayele et al., 2021; Coronavirus, 2022]. These therapeutics are exemplified by molnupiravir, nirmatrelvir and remdesivir. Nirmatrelvir inhibits SARS-CoV-2 replication by covalently targeting the viral main protease (M^{pro}) [Imran et al., 2021]. Nirmatrelvir undergoes oxidation by cytochrome P450s and the oxidation represents inactivation (CYPs, Gandhi et al., 2020). Molnupiravir and remdesivir, on the other hand, inhibit viral replication by targeting RdRp (Table 2) [Malone and Campbell, 2021; Zhang et al., 2021]. Remdesivir causes RdRp to pause or induces chain termination, whereas molnupiravir causes RdRp to introduce widespread errors, leading to lethal mutagenesis. They are ester prodrugs, molnupiravir is hydrolyzed by CES2 and remdesivir by CES1 (Figs. 2 and 3) [Shen et al., 2021a]. In addition, remdesivir is a potent and irreversible CES2 inhibitor [Shen et al., 2021b]. In addition to hydrolysis, remdesivir undergoes oxidation [Gandhi et al., 2022], but it remains to be determined whether oxidation is involved in the metabolism of molnupiravir. Phosphorylation is nevertheless required to produce therapeutically active metabolite for both drugs. Three-steps of phosphorylation are required for molnupiravir but only two-steps for remdesivir [Imran et al., 2021; Yan et al., 2021]. Molnupiravir is taken orally, whereas remdesivir intravenously (Table 2). Finally, both drugs and their metabolites are effective against major variants of SARS-CoV-2 (Table 3) [Vangeel et al., 2022], although the relative potency varies depending on a parent drug or a metabolite.

Molnupiravir and its hydrolytic metabolite N-hydroxycytidine [Kabinger et al., 2021] have much lower potency than remdesivir and its major metabolite (Table 3). According to the EC_{50} values (concentration effective in producing 50% of viral inhibition), molnupiravir is less effective than

DMD Fast Forward. Published on July 5, 2022 as DOI: 10.1124/dmd.122.000918
This article has not been copyedited and formatted. The final version may differ from this version.

its metabolite N-hydroxycytidine by 57-77% depending on a strain of SARS-CoV-2. In contrast, remdesivir is much more effective than GS-441524, a major metabolite of remdesivir [Vangeel et al., 2022]. Actually, remdesivir is ~10 times of the potency of GS-441524 against almost all SARS-CoV-2 variants (Table 3). It is well established that these metabolites undergo direct phosphorylation to produce the therapeutically active metabolites for both molnupiravir and remdesivir [Imran et al., 2021; Yan et al., 2021 28-30]. The differences in the relative EC_{50} values between the parent drugs (molnupiravir and remdesivir) and their metabolites point to the efficiency of cell membrane crossing and intracellular activation of the parent drugs (e.g., hydrolysis).

Membrane crossing is mediated by passive diffusion and active transport [King, 1996]. Remdesivir and its major metabolite GS-441524 have an XLogP3 value of -1.4 and +1.9, respectively. These values constitute a relatively large net difference (i.e., 3.3), suggesting passive diffusion favoring remdesivir over GS-441524 for membrane-crossing. Remdesivir undergoes hydrolysis by CES1 and is eventually converted to GS-441524 [Shen et al., 2021a]. The significantly higher efficacy of remdesivir than GS-441524 points to rapid diffusion and efficient hydrolysis in the SARS-CoV-2 infected cells. In contrast, molnupiravir and its hydrolytic metabolite N-hydroxycytidine have an XLogP3 value of -0.8 and -2.2, resulting in a relatively small net difference (i.e., 1.4). Such difference points to an involvement of both passive and active transport. Based on their respective XLogP3 values, N-hydroxycytidine is actively transported more than the parent drug molnupiravir. Indeed, drug transporters such as equilibrative nucleoside transporters 1 and 2 (ENT1 and ENT2), common uptake transporters, have been indicated to facilitate the membrane crossing of N-hydroxycytidine [Miller et al., 2021]. Interestingly, remdesivir is a substrate of these two transporters as well [Miller et al., 2021].

DMD Fast Forward. Published on July 5, 2022 as DOI: 10.1124/dmd.122.000918
This article has not been copyedited and formatted. The final version may differ from this version.

It is therefore suggested that remdesivir likely impacts the efficacy of molnupiravir through at least two mechanisms: transport and hydrolysis. In a cell model, remdesivir inhibits ENT1 uptake at an IC_{50} of 39 μM (the half maximal inhibitory concentration) and ENT2 at an IC_{50} of 77 μM [Miller et al., 2021]. In contrast, N-hydroxycytidine inhibits ENT1 uptake at an IC_{50} of 259 μM and ENT2 at 467 μM. Remdesivir is 6 times as potent as N-hydroxycytidine toward both transporters. Clinical trials have reported Cmax of 4.1 μM for remdesivir and 14.0 μM for N-hydroxycytidine [Deb et al., 2021; Painter et al., 2021], pointing to potential uptake interactions if they are co-present at similar time-frame. In this study, we have shown that molnupiravir is hydrolytically activated by CES2 and the activation is potently inhibited by remdesivir, a potent and irreversible CES2 inhibitor [Shen et al., 2021b]. The inhibition occurs in primary hepatocytes and with microsomal preparations from the intestine, liver and kidney (Figs. 5 and 6). Interestingly, the inhibition is the highest with the intestinal microsomes but least with liver microsomes (Fig. 4A). It is likely that liver microsomes have high levels of CES1, which robustly hydrolyzes remdesivir, leading to decreased inhibitory potency of remdesivir. In support of this possibility, liver microsomes contain higher levels of CES1 over CES2 based on native-gel electrophoresis coupled activity staining (Middle of Fig. 4A), but the relative staining intensity between CES1 and CES2 is reversed with lysates from primary hepatocytes (Fig. 5A). We have determined the inhibition of CES2 by remdesivir in the presence of increasing CES1. As predicated, increasing CES1 leads to decreased inhibition of CES2.

While it cannot be completely excluded that liver microsomes have another enzyme(s) that hydrolyzes molnupiravir, CES2 is nevertheless the predominately enzyme for molnupiravir hydrolysis. Several lines of evidence support this possibility. Microsomes from multiple organs, with an exception of the lung, show robust hydrolysis of molnupiravir and the relative magnitude of hydrolysis is related to the level of CES2 expression (Fig. 3A). The antiviral activity of N-hydroxycytidine in the lung is presumably achieved by active uptakes. Alveolar epithelial cells

DMD Fast Forward. Published on July 5, 2022 as DOI: 10.1124/dmd.122.000918
This article has not been copyedited and formatted. The final version may differ from this version.

have been reported to express high levels of ENT1 and ENT2, uptake transporters for N-hydroxycytidine [Painter et al., 2021; Baba et al., 2021]. Similarly, a large number of liver microsomal samples show high levels of correlation between the hydrolysis of molnupiravir and the expression of CES2 (Fig. 2B). There are nonetheless outliers, pointing to potential CES2 polymorphisms toward molnupiravir. Indeed, we have shown that the CES2 variant E485V is approximately half active as the wild-type, and conversely, the variant R180H is almost twice as active as the wild-type (Fig. 6A). And finally, remdesivir, an irreversible CES2 inhibitor (Shen at al., 2021b), efficaciously inhibits molnupiravir hydrolysis (Figs. 4 and 5).

In addition to altered molnupiravir hydrolysis, CES2 genetic variants show differences in the sensitivity to remdesivir inhibition. At 0.1 μM, remdesivir inhibits the wild-type CES2 by as much as 87% of molnupiravir hydrolysis. However, the same concentration inhibits genetic variants from 55 to 77% depending on a variant (Fig. 6B). On the other hand, remdesivir at 1 μM comparably inhibits the wild-type and all variants for the hydrolysis of molnupiravir, 90% or higher (Fig. 6B). One explanation is that these variants do not have significantly structural changes toward remdesivir. Indeed, molecular docking study has shown that remdesivir interacts with wild-type CES2 and its variant R180H through the same with an exception of 3 amino acids (out of 20) including A257, S266 and L381 (Table 1). In contrast, wild-type CES2 and its variant R180H differ by as many as 9 amino acids in the interaction with molnupiravir. It is likely that these amino acids of the variant R180H favor interactions with molnupiravir, thus leading to a large increase of molnupiravir hydrolysis (Fig. 6A).

It is interesting to notice that molnupiravir and remdesivir share as many as 13 amino acids in the interaction with the wild-type CES2 (Fig. 7, Table 1), although both drugs structurally differ greatly (Fig. 1A) [Shen et al., 2021b]. In addition, all shared residues, with exceptions of 5 amino acids only, use the same types of interaction (e.g., hydrogen bond) (Fig. 7, Table 1).

DMD Fast Forward. Published on July 5, 2022 as DOI: 10.1124/dmd.122.000918
This article has not been copyedited and formatted. The final version may differ from this version.

These findings suggest that both substrate (molnupiravir) and inhibitor (remdesivir) use similar ways to interact with CES2. All carboxylesterases nevertheless use the triad (Ser-His-Glu) for hydrolysis [Holmes et al., 2010; Shen et al., 2019; Yan, 2012]. This catalytic machinery follows two steps; formation of the drug-carboxylesterase complex (step one) following the hydrolysis of the complex via an activated water molecule (step two). The velocity of step two determines if an ester is a substrate (fast) or inhibitor (slow). It is therefore that modification of a substrate likely leads to an identification of an inhibitor or vice versa.

In summary, our work points to several important conclusions. First, molnupiravir is a substrate of CES2 but not CES1. Second, the hydrolysis of molnupiravir varies among CES2 natural variants, pointing to genetic polymorphisms for molnupiravir hydrolytic activation. Third, molnupiravir hydrolysis is profoundly inhibited by remdesivir, pointing to the potential of interfering with activation of molnupiravir. This possibility is reasonably high as the inhibition by remdesivir is achieved through irreversible CES2 inhibition. On the other hand, it is not clear how long the activity of CES2 can be restored *in vivo*, most likely through newly translated CES2. Remdesivir is an intravenous agent, creating uncertainties on the magnitude of organ-specific inhibition (e.g., liver versus intestine). Remdesivir and N-hydroxycytidine share transporters, further increasing the complexity of the interaction. Clinical trials are needed to establish the precise magnitude of remdesivir-molnupiravir interaction.

DMD Fast Forward. Published on July 5, 2022 as DOI: 10.1124/dmd.122.000918
This article has not been copyedited and formatted. The final version may differ from this version.

5. AUTHORSHIP CONTRIBUTIONS

Participated in research design: BY, YS

Conducted experiments: YS, WE, WL

Performed data analysis: YS, We

Wrote or contributed to the writing of the manuscript: BY, YS

DMD Fast Forward. Published on July 5, 2022 as DOI: 10.1124/dmd.122.000918
This article has not been copyedited and formatted. The final version may differ from this version.

6. REFERENCES

Asif Z, Chen Z, Stranges S, Zhao X, Sadiq R, Olea-Popelka F, Peng C, Haghighat F, Yu T (2022) Dynamics of SARS-CoV-2 spreading under the influence of environmental factors and strategies to tackle the pandemic: A systematic review. *Sustain Cities Soc*. **81**:103840.

Ayele AG, Enyew EF, Kifle ZD (2021) Roles of existing drug and drug targets for COVID-19 management. *Metabol Open*. **11:**100103.

Baba S, Yumoto R, Kawami M, Takano M (2021) Functional expression of equilibrative and concentrative nucleoside transporters in alveolar epithelial cells. *Pharmazie*. **76:**416-421.

Bienert S, Waterhouse A, de Beer TA, Tauriello G, Studer G, Bordoli L, Schwede T. (2017) The SWISS-MODEL Repository-new features and functionality. *Nucleic Acids Res*. **45**:D313-D319.

Bojkova D, Widera M, Ciesek S, Wass MN, Michaelis M, Cinatl J Jr (2022) Reduced interferon antagonism but similar drug sensitivity in Omicron variant compared to Delta variant of SARS-CoV-2 isolates. *Cell Res*. **21**:1–3.

COVID-19 Dashboard (2022) https://covid19.who.int/ WHO Coronavirus (COVID-19) Dashboard

COVID-19 Vaccines (2022) https://www.yalemedicine.org/news/covid-19-vaccine-comparison. Comparing the COVID-19 Vaccines: How Are They Different?

Coronavirus Treatment Acceleration Program (CTAP) (2022) https://www.fda.gov/drugs/coronavirus-covid-19-drugs/coronavirus-treatment-acceleration-program-ctap.

Deb S, Reeves AA, Hopefl R, Bejusca R (2021) ADME and Pharmacokinetic Properties of Remdesivir: Its Drug Interaction Potential. *Pharmaceuticals (Basel)*. 14:655.

Eng H, Dantonio AL, Kadar EP, Obach RS, Di L, Lin J, Patel NC, Boras B, Walker GS, Novak JJ, Kimoto E, Singh RSP, Kalgutkar AS (2022) Disposition of Nirmatrelvir, an Orally Bioavailable Inhibitor of SARS-CoV-2 3C-Like Protease, across Animals and Humans. *Drug Metab Dispos.* **50**:576-590.

Gandhi Z, Mansuri Z, Bansod S (2022) Potential Interactions of Remdesivir with Pulmonary Drugs: a COVID-19 Perspective. *SN Compr Clin Med*. **2**:1707-1708.

Getz WM, Salter R, Luisa Vissat L, Koopman JS, Simon CP (2021) A runtime alterable epidemic model with genetic drift, waning immunity and vaccinations. *J R Soc Interface*. **18**:20210648.

Holmes R, Wright M, Laulederkind S, Cox L, Hosokawa M, Imai T, Ishibashi S, Lehner R, Miyazaki M, Potter P, Redinbo M, Robert J, Satoh T, Yamashita T, Yan B, Yokoi T, Rudolf-Zechner R, Maltais L (2010) Recommended nomenclature for five mammalian

carboxylesterase gene families: Human, mouse and rat Genes and proteins. *Mammalian Genome*. **21**:427-441.

Huang HC, Lai YJ, Liao CC, Yang WF, Huang KB, Lee IJ, Chou WC, Wang SH, Wang LH, Hsu JM, Sun CP, Kuo CT, Wang J, Hsiao TC, Yang PJ, Lee TA, Huang W, Li FA, Shen CY, Lin YL, Tao MH, Li CW (2021) Targeting conserved N-glycosylation blocks SARS-CoV-2 variant infection in vitro. *EBioMedicine*. **74**:103712.

Imran M, Kumar Arora M, Asdaq SMB, Khan SA, Alaqel SI, Alshammari MK, Alshehri MM, Alshrari AS, Mateq Ali A, Al-Shammeri AM, Alhazmi BD, Harshan AA, Alam MT, Abida (2021) Discovery, development, and patent trends on molnupiravir: A Prospective Oral Treatment for COVID-19. *Molecules*. **26**:5795.

Jia Z, Gong W (2021) Will mutations in the Spike protein of SARS-CoV-2 lead to the failure of COVID-19 vaccines? *J Korean Med Sci*. **36**:e124.

Kabinger F, Stiller C, Schmitzová J, Dienemann C, Kokic G, Hillen HS, Höbartner C, Cramer P (2021) Mechanism of molnupiravir-induced SARS-CoV-2 mutagenesis. *Nat Struct Mol Biol*. **28**:740-746.

King RB (1996) Modeling membrane transport. *Adv Food Nutr Res*. **40**:243-62.

Lipsitch M, Krammer F, Regev-Yochay G, Lustig Y, Balicer RD (2021) SARS-CoV-2 breakthrough infections in vaccinated individuals: measurement, causes and impact. *Nat Rev Immunol*. **7**:1–9.

Malone B, Campbell EA (2021) Molnupiravir: coding for catastrophe. *Nat Struct Mol Biol*. **28**:706-708.

Mansbach RA, Chakraborty S, Nguyen K, Montefiori DC, Korber B, Gnanakaran S (2021) The SARS-CoV-2 Spike variant D614G favors an open conformational state. *Sci Adv*. **7**:eabf3671.

Miller SR, McGrath ME, Zorn KM, Ekins S, Wright SH, Cherrington NJ (2021) Remdesivir and EIDD-1931 interact with human equilibrative nucleoside transporters 1 and 2: Implications for reaching SARS-CoV-2 viral sanctuary sites. *Mol Pharmacol*. **100**:548-557.

Morris GM, Huey R, Lindstrom W, Sanner MF, Belew RK, Goodsell DS, Olson AJ (2009) AutoDock4 and AutoDockTools4: Automated docking with selective receptor flexibility. *J Comput Chem*. **30**:2785-91.

Muhammed Y, Yusuf Nadabo A, Pius M, Sani B, Usman J, Anka Garba N, Mohammed Sani J, Opeyemi Olayanju B, Zeal Bala S, Garba Abdullahi M, Sambo M (2021) SARS-CoV-2 spike protein and RNA dependent RNA polymerase as targets for drug and vaccine development: A review. *Biosaf Health*. **3**:249-263.

New Covid Pills Offer Hope as Omicron Looms at https://www.nytimes.com/2021/12/07/science/merck-pfizer-covid-pill-treatment.html

O'Boyle NM, Banck M, James CA, Morley C, Vandermeersch T, Hutchison GR (2011) Open Babel: An open chemical toolbox. *J Cheminform*. **3**:33.

Painter WP, Holman W, Bush JA, Almazedi F, Malik H, Eraut NCJE, Morin MJ, Szewczyk LJ, Painter GR (2021) Human safety, tolerability, and pharmacokinetics of molnupiravir, a novel broad-spectrum oral antiviral agent with activity against SARS-CoV-2. *Antimicrob Agents Chemother*. **65**:e02428-20.

Rosenke K, Hansen F, Schwarz B, Feldmann F, Haddock E, Rosenke R, Barbian K, Meade-White K, Okumura A, Leventhal S, Hawman DW, Ricotta E, Bosio CM, Martens C, Saturday G, Feldmann H, Jarvis MA (2021) Orally delivered MK-4482 inhibits SARS-CoV-2 replication in the Syrian hamster model. *Nat Commun*. **12**:2295.

Shapovalov MV, Dunbrack RL Jr (2011) A smoothed backbone-dependent rotamer library for proteins derived from adaptive kernel density estimates and regressions. *Structure*. **19**:844-58.

Shen Y, Yan B (2017) Covalent inhibition of carboxylesterase-2 by the anti-hepatitis C agent sofosbuvir: Implications in organ failures due to hydrolytic interactions with antiretroviral agents. *J Hepatol*. **66**:660-1.

Shen Y, Shi Z, Yan B (2019) Carboxylesterases: Pharmacological inhibition, regulated expression and transcriptional involvement of nuclear receptors and other transcription factors. *Nucl Receptor Res*. **6**:101435.

Shen Y, Shi Z, Fan JT, Yan B (2020) Dechlorination and demethylation of ochratoxin A enhance blocking activity of PXR activation, suppress PXR expression and reduce cytotoxicity. *Toxicol Lett*. **332**:171-180.

Shen Y, Eades W, Yan B (2021a) The COVID-19 Medicine Remdesivir Is Therapeutically Activated by Carboxylesterase-1, and Excessive Hydrolysis Increases Cytotoxicity. *Hepatol Commun*. **5**:1622-1623.

Shen Y, Eades W, Yan B (2021b) Remdesivir potently inhibits carboxylesterase-2 through covalent modifications: signifying strong drug-drug interactions. *Fundam Clin Pharmacol*. **35**:432-434.

Shi D, Yang J, Yang D, LeCluyse EL, Black C, You L, Akhlaghi F, Yan B (2006) Anti-influenza prodrug oseltamivir is activated by carboxylesterase HCE1 and the activation is inhibited by anti-platelet agent clopidogrel. *J Pharmacol Exp Ther*. **319**:1477-84.

Showers WM, Leach SM, Kechris K, Strong M (2021) Longitudinal analysis of SARS-CoV-2 spike and RNA-dependent RNA polymerase protein sequences reveals the emergence and geographic distribution of diverse mutations. *Infect Genet Evol*. **97**:105153.

Tang M, Mukundan M, Yang J, Charpentier N, LeCluyse EL, Black C, Yang D, Shi D, Yan B (2006) Antiplatelet agents aspirin and clopidogrel are hydrolyzed by distinct carboxylesterases, and clopidogrel is transesterificated in the presence of ethyl alcohol. *J Pharmacol Exp Ther*. **319**:1467-76.

Trott O, Olson AJ (2010) AutoDock Vina: improving the speed and accuracy of docking with a new scoring function, efficient optimization, and multithreading. *J Comput Chem*. **31**:455-61.

Vangeel L, Chiu W, De Jonghe S, Maes P, Slechten B, Raymenants J, André E, Leyssen P, Neyts J, Jochmans D (2022) Remdesivir, molnupiravir and nirmatrelvir remain active against SARS-CoV-2 Omicron and other variants of concern. *Antiviral Res*. **198**:105252.

Wagner R, Hildt E, Grabski E, Sun Y, Meyer H, Lommel A, Keller-Stanislawski B, Müller-Berghaus J, Cichutek K (2021) Accelerated development of COVID-19 vaccines: Technology platforms, benefits, and associated risks. *Vaccines (Basel)*. **9**:747.

Waters MD, Warren S, Hughes C, Lewis P, Zhang F (2022) Human genetic risk of treatment with antiviral nucleoside analog drugs that induce lethal mutagenesis - the special case of molnupiravir. *Environ Mol Mutagen*. **63**:37-63.

Wu MH, Yan B, Humerickhouse R, Dolan ME (2002) Irinotecan activation by human carboxylesterases in colorectal adenocarcinoma cells. *Clin Cancer Res*. **8**:2696-700.

Xiao D, Chen YT, Yang D, Yan B (2012) Age-related inducibility of carboxylesterases by the antiepileptic agent phenobarbital and implications in drug metabolism and lipid accumulation. *Biochem Pharmacol*. **84**:232-239.

Xiao D, Shi D, Yang D, Barthel B, Koch TH, Yan B (2013) Carboxylesterase-2 is a highly sensitive target of the antiobesity agent orlistat with profound implications in the activation of anticancer prodrugs. *Biochem Pharmacol*. **85**:439–47.

Xie M, Yang D, Liu L, Xue B, Yan B (2002) Human and rodent carboxylesterases: immuno-relatedness, overlapping substrate specificity, differential sensitivity to serine inhibitors, and tumor-related expression. *Drug Metab Dispos*. **30**:541-7.

Yan B. (2012) Hydrolytic enzymes, in Pavel Anzenbacher and Ulrich M. Zanger *Metabolism of Drugs and Other Xenobiotics* Wiley-VCH, Germany, pp 165-99.

Yan D, Ra OH, Yan B (2021) The nucleoside antiviral prodrug remdesivir in treating COVID-19 and beyond with interspecies significance. *Anim Dis*. **1**:15.

Zhang L, Zhang D, Wang X, Yuan C, Li Y, Jia X, Gao X, Yen HL, Cheung PP, Huang X (2021) 1'-Ribose cyano substitution allows Remdesivir to effectively inhibit nucleotide addition and proofreading during SARS-CoV-2 viral RNA replication. *Phys Chem Chem Phys*. **23**:5852-5863.

Zhao Y, Fang C, Zhang Q, Zhang R, Zhao X, Duan Y, Wang H, Zhu Y, Feng L, Zhao J, Shao M, Yang X, Zhang L, Peng C, Yang K, Ma D, Rao Z, Yang H (2021) Crystal structure of SARS-CoV-2 main protease in complex with protease inhibitor PF-07321332. *Protein Cell*. **22**:1–5.

Zhou YW, Xie Y, Tang LS, Pu D, Zhu YJ, Liu JY, Ma XL (2021) Therapeutic targets and interventional strategies in COVID-19: mechanisms and clinical studies. *Signal Transduct Target Ther*. **6**:317.

Zhu W, Song L, Matoney L, LeCluyse E, Yan B (2000) Dexamethasone differentially regulates the expression of carboxylesterase genes in humans and rats. *Drug Metab Dispos*. **28**:186-191.

DMD Fast Forward. Published on July 5, 2022 as DOI: 10.1124/dmd.122.000918
This article has not been copyedited and formatted. The final version may differ from this version.

7. FOOTNOTES

This work was partially supported by National Institutes of Health Grants R01EB018748 and R21AI153031 (Yan B).

The authors confirm the data that support the findings of this study are available from the corresponding author upon reasonable request. Some information may not be made available because of privacy or ethical restrictions.

Conflict of interest disclosure: None

DMD Fast Forward. Published on July 5, 2022 as DOI: 10.1124/dmd.122.000918
This article has not been copyedited and formatted. The final version may differ from this version.

LEGENDS FOR FIGURES

Fig. 1. Structure and elution profile of molnupiravir and its hydrolytic metabolite N-hydroxycytidine. (A) Structure of molnupiravir. **(B)** Structure of N-hydroxycytidine. **(C)** Elution profile of molnupiravir. And **(D)** Elution profile of N-hydroxycytidine. Representative chromatograms of molnupiravir (0.6 ng) and N-hydroxycytidine (0.18 ng) eluted with a gradient mobile phase constituting ammonium acetate (1 mM, pH 4,3) in water and acetonitrile as described in the text.

Fig. 2. Hydrolysis of molnupiravir by individual human liver samples and correlation analysis of the hydrolysis with the level of CES1 or CES2. (A) Molnupiravir hydrolysis by individual liver samples. Liver S9 fractions (2 μg) were incubated with molnupiravir at a final concentration of 1 μM for 40 min and the formation of the hydrolytic metabolite N-hydroxycytidine was analyzed by LC-MS/MS. For Western blotting, S9 fractions (3 μg) were subjected to SDS-polyacrylamide gel electrophoresis, electrophoretically transferred to nitrocellulose membrane and detected by the chemiluminescent detection system for CES1, CES2 or GAPDH. **(B)** Correlation between molnupiravir hydrolysis and the level of CES2 or CES1. The intensity of immunostaining was captured and quantified by ChemiDoc Imaging system. The immunostaining intensity of CES1 or CES2 was plotted against the relative hydrolysis of molnupiravir. The correlation coefficient and the corresponding p vales were calculated. An arrow sign indicates potential outliers. **(C)** Correlation between CES1 and CES2 expression. Statistical significance of correlation at $p < 0.01$

Fig. 3. Hydrolysis of molnupiravir by organ-specific microsomes and cell lysates containing recombinant CES1 or CES2. (A) Molnupiravir hydrolysis by organ-specific microsomes. Pooled microsomes (2 μg) from the intestine (n = 6), liver (n = 20), kidney (n = 20) or lung (n = 10) were incubated with molnupiravir at a final concentration of 1 μM for 40 min and

DMD Fast Forward. Published on July 5, 2022 as DOI: 10.1124/dmd.122.000918
This article has not been copyedited and formatted. The final version may differ from this version.

the formation of the hydrolytic metabolite N-hydroxycytidine was analyzed by LC-MS/MS. For Western blotting, microsomes (1.2 μg) were subjected to SDS-polyacrylamide gel electrophoresis, electrophoretically transferred to nitrocellulose membrane and detected by the chemiluminescent detection system for CES1, CES2, GAPDH or β-actin. Single asterisk for statistical significance at $p < 0.05$, double at $p < 0.01$ and triple at $p < 0.001$ based on the comparison from the hydrolysis by intestinal microsomes. **(B)** Representative chromatogram of molnupiravir hydrolysis by pooled microsomes from the intestine (MPV: molnupiravir, NHC: N-hydroxycytidine). **(C)** Molnupiravir hydrolysis by cell lysates containing recombinant CES1 or CES2. Cells (293T) were transfected by CES1, CES2 or the corresponding vector. Cell lysates (0.1 μg) were tested for the hydrolysis of molnupiravir hydrolysis. Western blotting confirmed the expression of CES1 and CES2 upon transfection. Triple asterisks for statistical significance at $p < 0.001$ from vector control.

Fig. 4. Remdesivir-inhibition of molnupiravir hydrolysis in microsomes. **(A)** Selective inhibition of CES2 by remdesivir. Pooled microsomes (2 μg) from the intestine (n = 6), liver (n = 20) and kidney (n = 20) were incubated with remdesivir (RDV at 0, 1 or 10 μM) for 2 h, and then subjected to native gel electrophoresis. The gel was then stained for esterase activity by 4-methylumbelliferyl acetate. Images were captured by ChemiDoc Imaging system. **(B)** Inhibition of molnupiravir hydrolysis. Pooled microsomes (2 μg) were incubated with remdesivir (RDV) for 2 h and then with 1 μM molnupiravir for 40 min. The hydrolysis of molnupiravir was monitored for the production of the formation of N-hydroxycytidine was analyzed by LC-MS/MS. Single asterisk for statistical significance at $p < 0.05$, double at $p < 0.01$ and triple at $p < 0.001$ for the comparison indicated by a line.

Fig. 5. Remdesivir-inhibition of molnupiravir hydrolysis in microsomes. **(A)** Intracellular inhibition of CES2 by remdesivir (RDV) with 4-methylumbelliferylacetate as the substrate.

DMD Fast Forward. Published on July 5, 2022 as DOI: 10.1124/dmd.122.000918
This article has not been copyedited and formatted. The final version may differ from this version.

Human primary hepatocytes suspension (10^6) were incubated with RDV at various concentrations (0, 1 or 10 μM) for 2 h and then centrifuged at 1000 *g* and washed extensively. The hepatocytes were then lysed and analyzed for CES2 inhibition by native gel electrophoresis. **(B)** Intracellular inhibition of molnupiravir hydrolysis by RDV with molnupiravir as the substrate. Human primary hepatocytes suspension (10^6) were incubated with RDV at various concentrations (0, 1 or 10 μM) for 2 h and washed as above. The pellets were resuspended and then incubated with molnupiravir at 1 μM for 40 min. The formation of N-hydroxycytidine by LC-MS/MS. Single asterisk denotes statistical significance at $p < 0.05$, double at $p < 0.01$ and triple at $p < 0.001$ for the comparison indicated by a line.

Fig. 6. Hydrolysis of molnupiravir by CES2 polymorphic variants and inhibited hydrolysis by remdesivir. **(A)** Hydrolysis of molnupiravir by CES2 polymorphic variants. Cells (293T) were transfected by the wild-type CES2 or mutant. Cell lysates (0.5 μg) were tested for the hydrolysis of molnupiravir hydrolysis. The same amount of lysates was analyzed by Western blotting for the expression. The hydrolysis was normalized based on the intensity of the immunostaining. Single asterisk denotes statistical significance at $p < 0.05$ and double at $p < 0.01$ for the comparison with the wild-type CES2. **(B)** Remdesivir-inhibited hydrolysis of molnupiravir by CES2 polymorphic variants. Lysates (0.5 μg) from transfected cells were incubated with remdesivir (RDV) at 0, 0.1, 1 and 10 μM for 2 h and then with 1 μM molnupiravir for 40 min. The hydrolysis of molnupiravir was monitored for the production of the formation of N-hydroxycytidine was analyzed by LC-MS/MS. Single asterisk denotes statistical significance at $p < 0.05$, double at $p < 0.01$ and triple at $p < 0.001$ for the comparison indicated by a line.

Fig. 7. Molecular docking of molnupiravir, remdesivir and sofosbuvir The molecular docking was performed by Autodock Vina. The ligands were sourced from PubChem as 3-D spatial data files. The wild-type CES2 was downloaded from the PDB and Swiss Model

DMD Fast Forward. Published on July 5, 2022 as DOI: 10.1124/dmd.122.000918
This article has not been copyedited and formatted. The final version may differ from this version.

websites and cleaned to remove the ligand and any other unwanted molecules such as water using the Chimera. The CES2 mutants were generated in the Chimera with the rotamer function. These files were then prepared for simulation by Autodock Tools. The center for the Autodock Vina simulation was the center of CES2 or its mutants. The search box was set to 126 x 126 x 126 with an exhaustiveness of 100.

Table 1. Contact amino acids of CES2 or R180H variant with molnupiravir (MPV) or remdesivir (RDV)

Interaction	Location of contact amino acids																							
MPV-CES2	L258	L259	P260	G261	H322	Q324	L378	L379	M380	S414	M415	I418	P419	Q422	W538	K539	L542							
RDV-CES2	L258	G261	I263	A264	S265	H322	Q324	L379	M380	L381	P382	S414	I418	P419	Q422	W538	K539	L542	Q544					
MPV-R180H	A257	L258	L259	L261	L262	I263	H322	P323	Q324	L379	M380	L381	S414	I418	P419	Q422	W538	L542						
RDV-R180H	A257	L258	G261	I263	A264	S265	S266	H322	Q324	L379	M380	P382	S414	I418	P419	Q422	W538	K539	L542	Q544				

DMD Fast Forward. Published on July 5, 2022 as DOI: 10.1124/dmd.122.000918
This article has not been copyedited and formatted. The final version may differ from this version.

Table 2. Comparison and contrast between molnupiravir and remdesivir

Item	Molnupiravir	Remdesivir
Target	RdRp	RdRp
Consequence	Errors introduced	Pausing/termination
Hydrolysis	Required (CES2)	Required (CES1)
Covalent inhibition		CES2
Oxidation	?	Yes
Phosphorylation	Required	Required
Dosage regimens	800 mg/twice/12 h	100 mg/day
Giving route	Oral	Intravenous

RdRp, RNA-dependent RNA-polymerase; CES1 or 2, carboxylesterase-1 or 2

DMD Fast Forward. Published on July 5, 2022 as DOI: 10.1124/dmd.122.000918
This article has not been copyedited and formatted. The final version may differ from this version.

Table 3. Half maximal effective concentration (EC_{50}) against SARS-CoV-2 variants

Drug/metabolite	Alpha	Beta	Gamma	Delta	Omicron	GHB
Molnupiravir	3.6				1.9	3.9
NHC	2.3	1.5	2.0	3.3		2.2
Remdesivir	0.077	0.063	0.074		0.048	0.052
GS-441524	0.76	0.77	0.90	0.87	0.50	0.81

NHC: β-d-N4-hydroxycytidine, hydrolytic metabolite of molnupiravir; GS-441524: major metabolite of remdesivir in the blood. Vangeel et al., Antiviral Res. 2022, 198:105252.

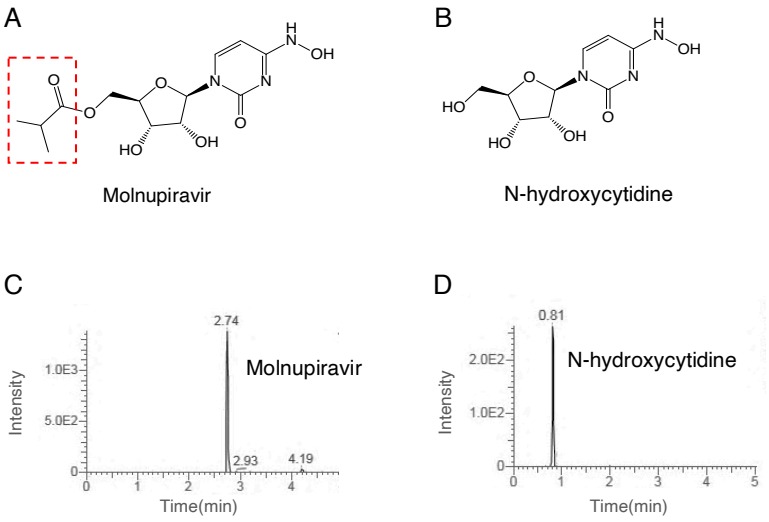
A
B
Molnupiravir
N-hydroxycytidine
C
D
2.74
Molnupiravir
2.93
4.19
Intensity
1.0E3
5.0E2
Time(min)
0.81
N-hydroxycytidine
2.0E2
1.0E2

Figure 1

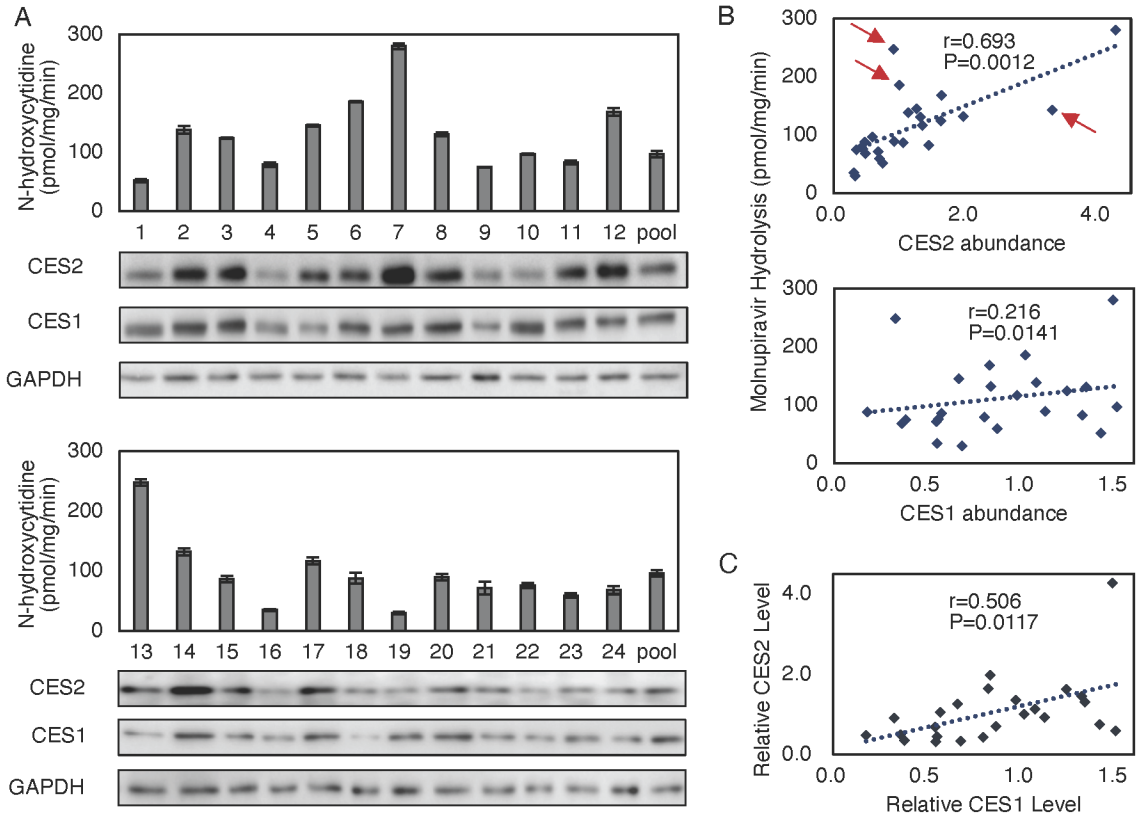
A
N-hydroxycytidine (pmol/mg/min)
300
200
100
0
1 2 3 4 5 6 7 8 9 10 11 12 pool
CES2
CES1
GAPDH
N-hydroxycytidine (pmol/mg/min)
300
200
100
0
13 14 15 16 17 18 19 20 21 22 23 24 pool
CES2
CES1
GAPDH
B
Molnupiravir Hydrolysis (pmol/mg/min)
300
200
100
0
r=0.693
P=0.0012
0.0 2.0 4.0
CES2 abundance
300
200
100
0
r=0.216
P=0.0141
0.0 0.5 1.0 1.5
CES1 abundance
C
Relative CES2 Level
4.0
2.0
0.0
r=0.506
P=0.0117
0.0 0.5 1.0 1.5
Relative CES1 Level

Figure 2

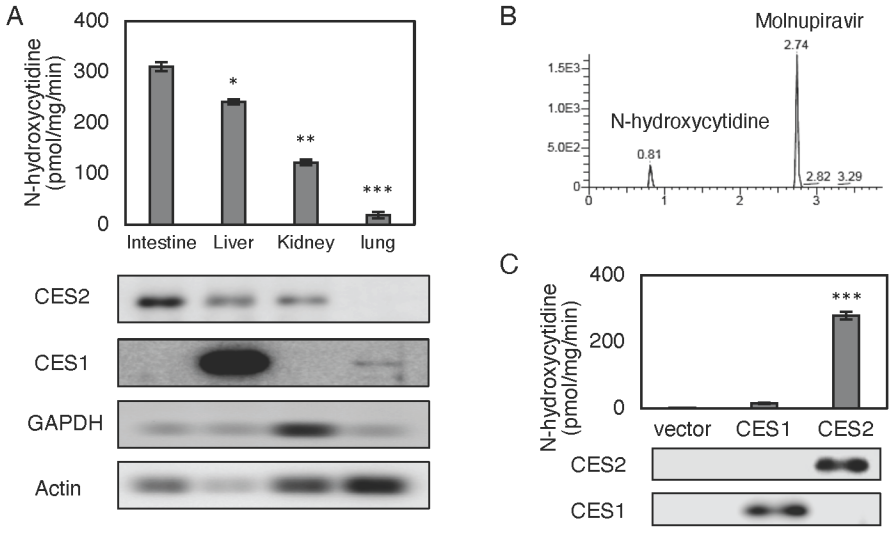
A
400
300
200
100
0
N-hydroxycytidine (pmol/mg/min)
*
**
***
Intestine
Liver
Kidney
lung
CES2
CES1
GAPDH
Actin
B
Molnupiravir
2.74
1.5E3
1.0E3
5.0E2
0
N-hydroxycytidine
0.81
2.82
3.29
0
1
2
3
C
400
200
0
N-hydroxycytidine (pmol/mg/min)
***
vector
CES1
CES2
CES2
CES1

Figure 3

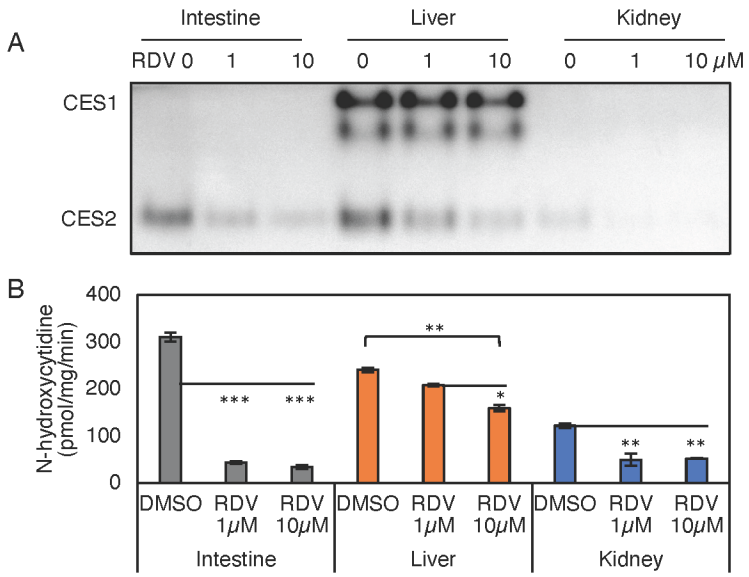
A
Intestine
Liver
Kidney
RDV 0
1
10
0
1
10
0
1
10 μM
CES1
CES2
B
N-hydroxycytidine (pmol/mg/min)
400
300
200
100
0
***
***
**
*
**
**
DMSO
RDV 1μM
RDV 10μM
Intestine
Liver
Kidney

Figure 4

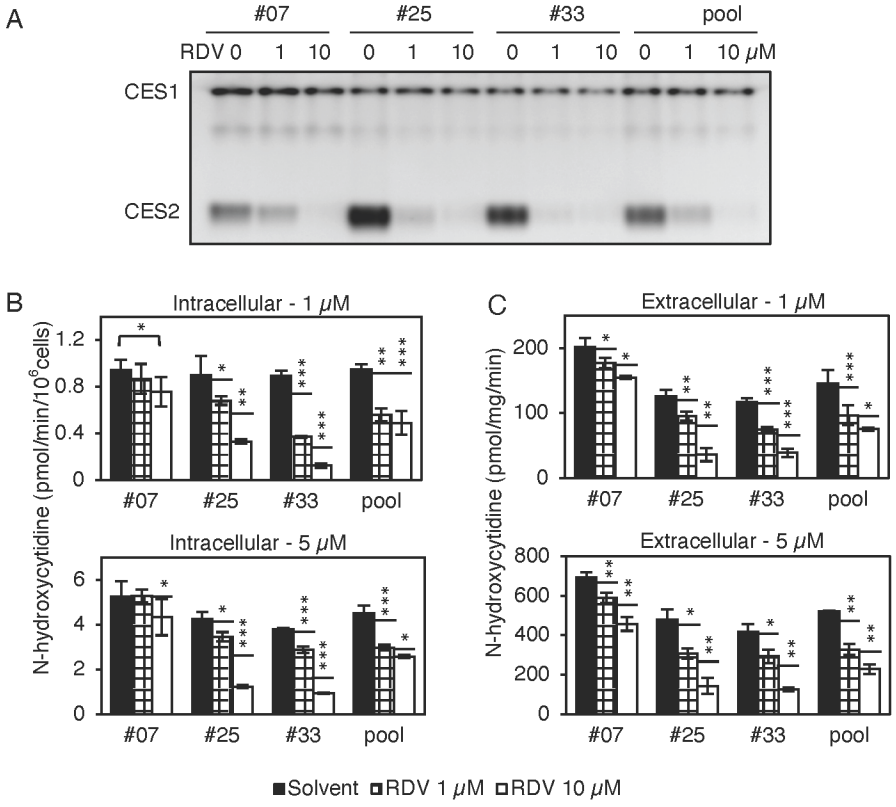
A
#07
#25
#33
pool
RDV 0 1 10 0 1 10 0 1 10 0 1 10 μM
CES1
CES2
B
Intracellular - 1 μM
N-hydroxycytidine (pmol/min/10^6cells)
1.2
0.8
0.4
0
#07 #25 #33 pool
Intracellular - 5 μM
6
4
2
0
#07 #25 #33 pool
C
Extracellular - 1 μM
N-hydroxycytidine (pmol/mg/min)
200
100
0
#07 #25 #33 pool
Extracellular - 5 μM
800
600
400
200
0
#07 #25 #33 pool
Solvent RDV 1 μM RDV 10 μM

Figure 5

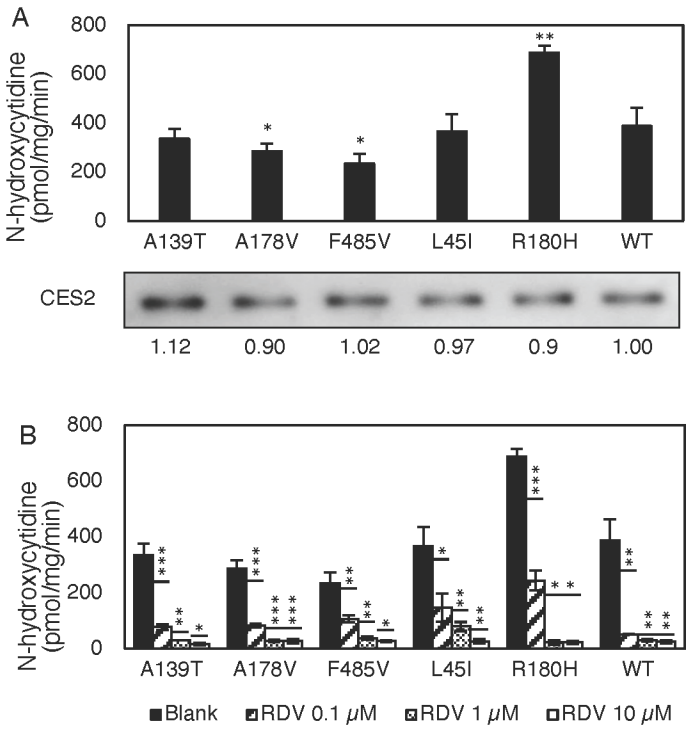
A
800
600
400
200
0
N-hydroxycytidine (pmol/mg/min)
A139T
A178V
F485V
L45I
R180H
WT
CES2
1.12
0.90
1.02
0.97
0.9
1.00
B
800
600
400
200
0
N-hydroxycytidine (pmol/mg/min)
A139T
A178V
F485V
L45I
R180H
WT
Blank
RDV 0.1 μM
RDV 1 μM
RDV 10 μM

Figure 6

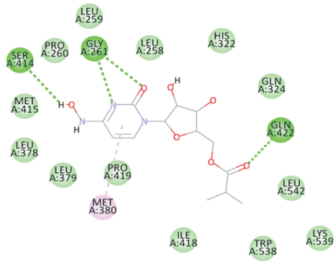

CES2-Molnupirivir

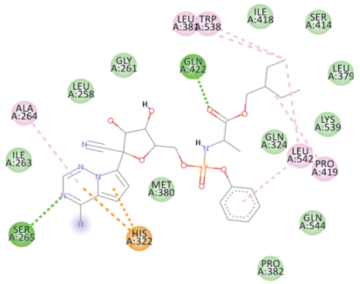

CES2-Remdesivir

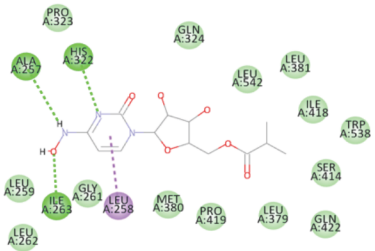

R180H-Molnupirivir

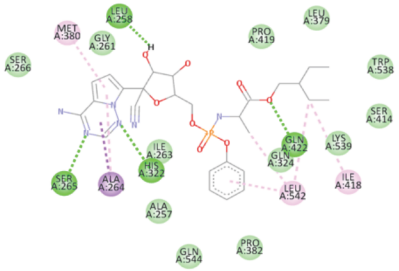

R180H-Remdesivir

Van der Waals | Hydrogen bond | Pi-Sigma | Pi-Alky | Pi-Cation

Figure 7